

Electromagnetic Hadron Form Factors: Status and Perspectives

E. Tomasi-Gustafsson¹, **G. I. Gakh**²

¹DAPNIA/SPhN, CEA/Saclay, 91191 Gif-sur-Yvette Cedex, France

²National Science Centre "Kharkov Institute of Physics and Technology"
61108 Akademicheskaya 1, Kharkov, Ukraine

Abstract.

An overview of the experimental data on nucleon form factors is presented in the space-like and in the time-like regions. A global description in the full kinematical region is done in terms of models developed in the space-like region and continued in the time-like region. The predictions of these models for polarization observables, which will be accessible in future with antiproton beams, are shown. Open problems and inconsistencies in the present data are also discussed.

1 Introduction

Electromagnetic hadron form factors (FFs) contain the information on the composite nature of hadrons. They are fundamental quantities which are directly accessible through the measurement of the differential cross section and of specific polarization observables. They enter in the expression of the electromagnetic current, and they are calculable by the models which describe the nucleon structure. Elastic electron hadron scattering is considered the most direct way to access FFs, which contain the information on the ground state of the hadron. Electromagnetic probes are traditionally preferred to hadronic probes and the interaction is assumed to occur through one photon exchange. In this case, FFs are real and functions of one variable, the four momentum squared of the virtual photon, $q^2 = -Q^2$. The interest in their measurement at large Q^2 is also related to the test of QCD predictions. FFs should give a clear signature of the transition region from a non perturbative description of the nucleon to a picture where quark and gluon degrees of freedom should be taken explicitly into account.

Due to the hermiticity of the hamiltonian, FFs are real in the space-like (SL) region and complex in the time-like region (TL). The TL region, where $q^2 > 0$,

is accessible through annihilation reactions, $p + \bar{p} \leftrightarrow e^+ + e^-$. Analyticity allows to relate the properties of FFs in all the kinematical region. We will show that it is possible, in frame of VDM models and QCD prescriptions as well, to find a reasonable description of the existing world data, and to make predictions on polarization observables in the TL region. Such data will be accessible in next future, with polarized antiproton beams planned at FAIR (GSI).

Large progress has been done in recent years in SL region, with the availability of the high intensity, high polarized electron beams, polarized targets, polarimeters, and large acceptance spectrometers, mainly at Jefferson Laboratory (JLab), and MAMI (Mainz). It has become possible to apply the polarization method, suggested many years ago [1], to extract the electric proton FF, with large precision up to $Q^2 = 5.6 \text{ GeV}^2$. Two dedicated experiments [2] (see the talk of V. Punjabi, this conference) showed that the ratio of the electric to the magnetic FF: $R = \mu_p G_{Ep}/G_{Mp}$ monotonically decreases and deviates from unity, as Q^2 increasing, reaching a value of $R \simeq 0.3$ at $Q^2 = 5.5 \text{ GeV}^2$. The following parametrization has been suggested:

$$R = \mu_p G_{Ep}/G_{Mp} = 1 - 0.13(Q^2 [\text{GeV}^2] - 0.04), \quad (1)$$

which shows that the electric and magnetic currents in the proton are different. This is a very surprising result, as all previous and also recent unpolarized measurements based on the Rosenbluth method [3] suggest that the ratio R is constant and consistent with unity. We will discuss further this inconsistency given by two methods which assume the same reaction mechanism and are formally consistent.

The magnetic proton FF has been measured up to $Q^2 = 31 \text{ GeV}^2$, assuming the scaling relation $R = 1$ for $Q^2 > 8.9 \text{ GeV}^2$ [4].

The polarization transfer method can be also applied to the neutron, but it needs deconvolution of nuclear effects for a deuteron or ^3He target. The neutron electric FF has been measured up to $Q^2 \simeq 1.5 \text{ GeV}^2$, and, although small, is not compatible with zero [5]. In the TL region, the measurement of the differential cross section for the processes $\bar{p} + p \leftrightarrow \ell^+ + \ell^-$ at a fixed value of the square of the total energy s and for two different angles of the scattered particle, θ , allows the separation of the two FFs, $|G_M|^2$ and $|G_E|^2$, and it is equivalent to the Rosenbluth separation for the elastic ep -scattering [6]. This procedure is simpler in TL region, as it requires to change only one kinematical variable, $\cos\theta$, whereas, in SL region, it is necessary to change simultaneously two kinematical variables: the energy of the initial electron and the electron scattering angle, fixing the momentum transfer squared.

In order to determine the form factors, the differential cross section has to be integrated over a wide angular range. One typically assumes that the G_E -contribution plays a minor role in the cross section at large momentum transfer and the experimental results are usually given in terms of $|G_M|$, under the hypothesis that $G_E = 0$ or $G_E = G_M$ [7].

Nucleon FFs in TL region are larger than in SL region. Neutron TL FFs have been measured only at Frascati [8]. These data, although they have larger errors, show that in TL region neutron FFs are larger than proton FFs.

2 Global description of the data

Different approaches have been developed for the description of the nucleon structure. However very few models exist, which can reproduce consistently all four nucleon form factors.

Few models predicted -at least qualitatively- the behavior of the electric proton FF, before the polarization data appeared. We quote here the VMD model from Ref. [9], the soliton model from Ref. [10], and, at a lesser extent, the diquark model from Ref. [11].

Not all models developed in SL region obey those analytical properties which allow their extension to TL region. The extension of the nucleon models developed for the SL region to the TL region is straightforward for VMD inspired models, which may give a good description of all FFs in the whole kinematical region, after a fitting procedure involving a certain number of parameters [12–14]. The parametrization [12] can be considered a successful generalization, in TL region, based on unitarity and analyticity. It requires the modelization of ten resonances, five isoscalar and five isovector.

Among the existing models of nucleon FFs, we consider some parametrizations, which have an analytical expression that can be continued in TL region: predictions of pQCD, in a form generally used as simple fit to experimental data, a model based on vector meson dominance (VMD) [9], and a third model based on an extension of VMD, with additional terms in order to satisfy the asymptotic predictions of QCD [15], in the form called GKex(02L). We also considered the Hohler parametrization [16] and the Bosted empirical fit [17].

The last two parametrizations can not be easily extended to TL region, as poles and instabilities appear in the physical region.

The analytical continuation to TL region is based on the following relations:

$$Q^2 = -q^2 = q^2 e^{-i\pi} \implies \begin{cases} \ln(Q^2) = \ln(q^2) - i\pi \\ \sqrt{Q^2} = e^{-\frac{i\pi}{2}} \sqrt{q^2} \end{cases} \quad (2)$$

Note that the sign of the phase may affect T-odd observables. Most of the models predict a different behavior for the electric and the magnetic FFs in TL region, whereas, as already mentioned, no individual determination of electric and magnetic FFs has been done yet due to the limited statistics which is possible to achieve¹. We chose to fit the data assuming that they correspond to the magnetic FFs for proton and neutron, Fig. 2a and 2c, respectively. Therefore, the curves for the electric FFs in Figs. 2b and 2d have to be considered predictions from the models. Including or not the data on neutron FFs, in TL region, influence very little the fitting procedure.

¹A recent analysis has been done in [18]

The parametrization from Ref. [9] is shown as a dotted line in Figs. 1 and 2. This model is based on a view of the nucleon as composed by an inner core with a small radius (described by a dipole term) surrounded by a meson cloud. While it reproduces very well the proton data in SL region (and particularly the polarization measurements), it fails in reproducing the large Q^2 behaviour of the magnetic neutron FF in SL region. The present fit constrained on the TL data and on the recent SL data does not improve the situation. In framework of this model a good global fit in SL region has been obtained with a modification including a phase in the common dipole term. However, the TL region is less well reproduced [14]. Therefore, the curves drawn in all the figures correspond to the original parameters, which give, in our opinion, a better representation of the whole set of data.

The result from an update fit based on the parametrization GKex(02L) [15] is shown in Figs. 1 and 2 (solid line). It is possible to find a good overall parametrization, with parameters not far from those found in the original paper

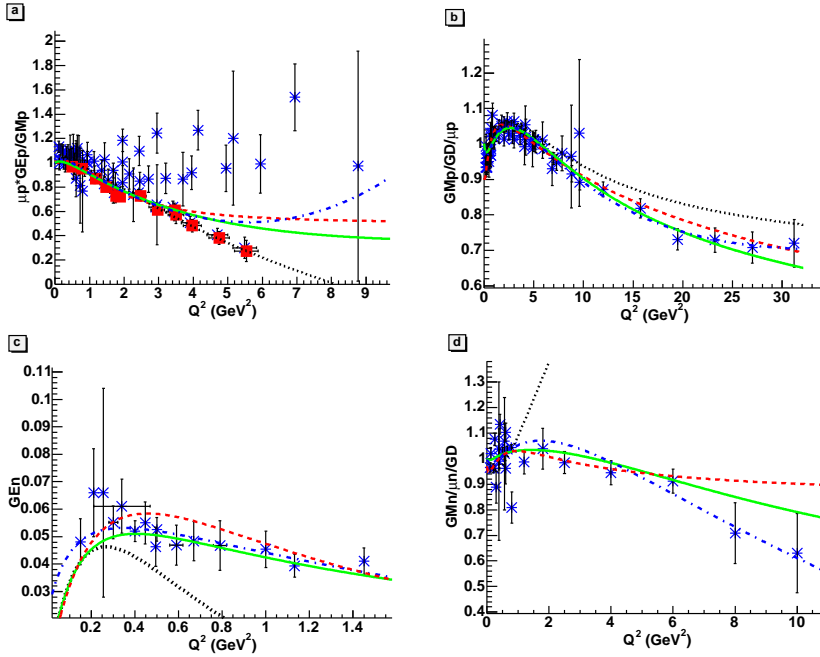


Figure 1. Nucleon Form Factors in Space-Like region: (a) proton electric FF, scaled by $\mu_p G_{Mp}$ (b) proton magnetic FF scaled by $\mu_p G_D$, (c) neutron electric FF, (d) neutron magnetic FF, scaled by $\mu_n G_D$. The predictions of the models are drawn: from Ref. [9] (dotted line), from Ref. [15] (solid line), model from Ref. [16] (dash-dotted line), from Ref. [17] (dashed line).

for the SL region only. The agreement is very good, for both proton and neutron FFs.

The pQCD prediction, based on counting rules, follows the dipole behavior in SL region, and can be extended in TL region as [19]:

$$|G_M| = \frac{A(N)}{q^4 \ln^2(q^2/\Lambda^2)}, \quad (3)$$

where $\Lambda = 0.3$ GeV is the QCD scale parameter and A is a free parameter. This simple parametrization is taken to be the same for proton and neutron. The best fit (Fig. 2, dashed line) is obtained with a parameter $A(p) = 56.3$ GeV⁴ for proton and $A(n) = 77.15$ GeV⁴ for neutron, which reflects the fact that in TL region neutron FFs are larger than proton ones. One should note that errors are also larger in TL region.

2.1 Observables in the TL region

The accessible observables in TL region, besides the differential cross section and the angular asymmetry, are single and double spin polarization observables.

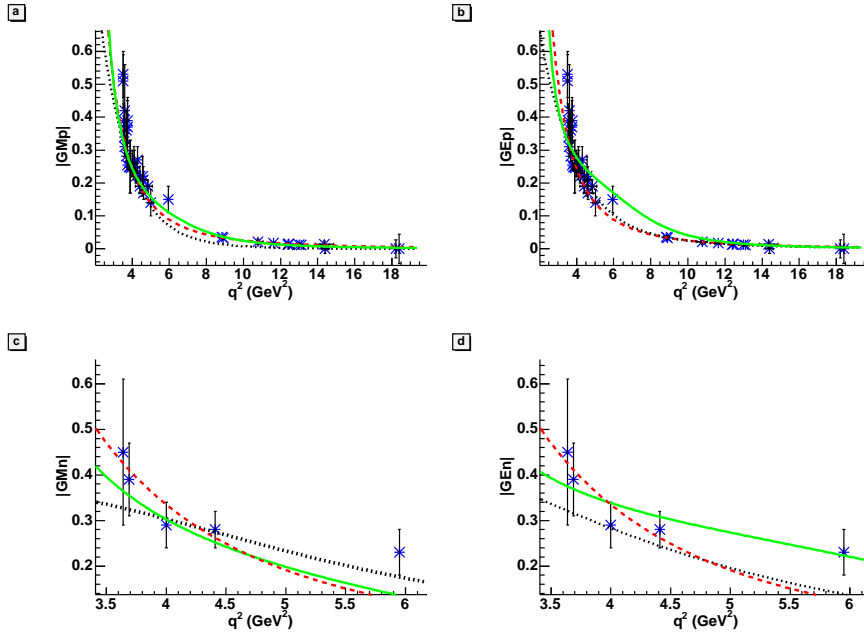


Figure 2. Form Factors in Time-Like region and predictions of the models: pQCD-inspired (dashed line), from Ref. [9] (dotted line), from Ref. [15] (solid line).

The differential cross section for the reaction $p + \bar{p} \rightarrow e^+ + e^-$ is written in the center of mass (CMS) as [6]:

$$\left(\frac{d\sigma}{d\Omega}\right)_0 = \mathcal{N} \left[(1 + \cos^2 \theta) |G_M|^2 + \frac{1}{\tau} \sin^2 \theta |G_E|^2 \right], \quad (4)$$

where $\mathcal{N} = \frac{\alpha^2}{4\sqrt{q^2(q^2 - 4m^2)}}$, $\alpha = e^2/(4\pi) \simeq 1/137$, is a kinematical factor.

The angular dependence of the cross section, Eq. (4), results directly from the assumption of one-photon exchange, where the photon has spin 1 and the electromagnetic hadron interaction satisfies the P -invariance. Therefore, the measurement of the differential cross section at three angles (or more) would also allow to test the presence of 2γ exchange [20].

The electric and the magnetic FFs are weighted by different angular terms, in the cross section, Eq. (4). One can define an angular asymmetry, \mathcal{R} , with respect to the differential cross section measured at $\theta = \pi/2$, σ_0 [21]:

$$\left(\frac{d\sigma}{d\Omega}\right)_0 = \sigma_0 [1 + \mathcal{R} \cos^2 \theta], \quad (5)$$

where \mathcal{R} can be expressed as a function of FFs:

$$\mathcal{R} = \frac{\tau |G_M|^2 - |G_E|^2}{\tau |G_M|^2 + |G_E|^2}. \quad (6)$$

This observable should be very sensitive to the different underlying assumptions on FFs, as it enhances the relative weight of the two angular terms.

The q^2 dependence of the total cross section can be presented as follows:

$$\sigma(q^2) = \mathcal{N} \frac{8}{3} \pi \left[2 |G_M|^2 + \frac{1}{\tau} |G_E|^2 \right]. \quad (7)$$

In case of polarized antiproton beam with polarization \vec{P}_1 , the only non zero analyzing power is related to P_y [6, 22, 23]:

$$\left(\frac{d\sigma}{d\Omega}\right)_0 A_{1,y} = \frac{\mathcal{N}}{\sqrt{\tau}} \sin 2\theta \text{Im}(G_M G_E^*). \quad (8)$$

If the target is polarized, again the terms related to $|G_E|^2$ and $|G_M|^2$ vanish and one can find $\vec{A}_2 = \vec{A}_1 = \vec{A}$, where the indices 1 and 2 refer to the projectile and the target, respectively. One can see that this analyzing power, being T-odd, does not vanish in $p + \bar{p} \rightarrow \ell^+ + \ell^-$, even in one-photon approximation, due to the fact that FFs are complex in time-like region. This is a principal difference with elastic ep scattering. Let us note also that the assumption $G_E = G_M$ implies $A_y = 0$, independently from any model taken for the calculation of

FFs. When both colliding particles are polarized, among the nine possible terms: $A_{xy} = A_{yx} = A_{zy} = A_{yz} = 0$ and the nonzero components are:

$$\begin{aligned}
 \left(\frac{d\sigma}{d\Omega}\right)_0 A_{xx} &= \sin^2 \theta \left(|G_M|^2 + \frac{1}{\tau} |G_E|^2 \right) \mathcal{N}, \\
 \left(\frac{d\sigma}{d\Omega}\right)_0 A_{yy} &= -\sin^2 \theta \left(|G_M|^2 - \frac{1}{\tau} |G_E|^2 \right) \mathcal{N}, \\
 \left(\frac{d\sigma}{d\Omega}\right)_0 A_{zz} &= \left[(1 + \cos^2 \theta) |G_M|^2 - \frac{1}{\tau} \sin^2 \theta |G_E|^2 \right] \mathcal{N}, \\
 \left(\frac{d\sigma}{d\Omega}\right)_0 A_{xz} &= \left(\frac{d\sigma}{d\Omega}\right)_0 A_{zx} = \frac{1}{\sqrt{\tau}} \sin 2\theta \operatorname{Re} G_E G_M^* \mathcal{N}, \quad (9)
 \end{aligned}$$

where A_{ab} are the spin correlation coefficients and the indices a and $b = x, y, z$ refer to the $a(b)$ component of the projectile (target) polarization. One can see that the double spin observables depend on the moduli squared of FFs, besides A_{xz} . Therefore, in order to determine the relative phase of FFs, in TL region, the interesting observables are A_y , and A_{xz} which contain, respectively, the imaginary and the real part of the product $G_E G_M^*$.

The predictions for the cross section asymmetry and the polarization observables can be done for those models, described above, which give a good overall description of the available FFs data in SL and TL regions. They are shown in Fig. 3, for a fixed value of $\theta = \pi/4$ (θ is the CMS angle between the antiproton and the outgoing electron). All these observables are, generally, quite large. The model [9] predicts the largest (absolute) value at $q^2 \simeq 15 \text{ GeV}^2$ for all observables, except A_{xz} , which has two pronounced extrema.

The observables manifest a different behavior, according to the different models. The sign, also, can be opposite for VMD inspired models and pQCD. The model [15] is somehow intermediate between the two representations, as it contains the asymptotic predictions of QCD (at the expenses of a larger number of parameters).

The fact that single spin observables in annihilation reactions are discriminative towards models, especially at threshold, was already pointed out in Ref. [22], for the process $e^+ + e^- \rightarrow p + \bar{p}$ on the basis of two versions of a unitary VMD model, and repeated more recently in Ref. [24]. The present results, (Fig. 3), for the inverse reaction $p + \bar{p} \rightarrow e^+ + e^-$, confirm this trend for all spin observables and show that experimental data will be extremely useful, particularly in the kinematical region around $q^2 \simeq 15 \text{ GeV}^2$ [25].

3 Asymptotic predictions

QCD scaling rules can predict the behavior (not the absolute value) of FFs, at large Q^2 . The elastic FF (in the interaction of a virtual photon with a hadron containing n quarks) is the probability that the hadron remains unchanged after transferring the momentum transfer squared to all components [19].

Assuming that the interaction is propagated by gluons (spin one particles) and conserving helicity, such probability can be written as

$$P_n = c_n/[1 + Q^2/n\beta^2]^{(n-1)} \quad (10)$$

where n is the number of constituent quarks and β is the average momentum of the quark. A value $\beta^2=0.471 \text{ GeV}^2$ can be determined from a fit to pion data (where $n = 2$). For the nucleon, proton and neutron as well, Eq. (10) reduced to the dipole formula

$$P_3 = c_3/[1 + Q^2(\text{GeV}^2)/.71]^2. \quad (11)$$

Note that, in non relativistic approach or in the Breit system, FFs are Fourier transform of the charge and magnetic distributions. Eq. (11) corresponds to the Fourier transform of an exponential distribution, and the value $.71 \text{ GeV}^2$ would result from a root mean square radius $\langle r^2 \rangle = 0.81 \text{ fm}^2$.

Electric FFs data issued from Rosenbluth measurements follow such scaling behavior for $Q^2 > 2 \text{ GeV}^2$, whereas polarization data do not. It has been recently shown that adding logarithmic correction [26] can reconcile recent data and QCD predictions. However those prescriptions are in contradiction with asymptotic properties following from analyticity.

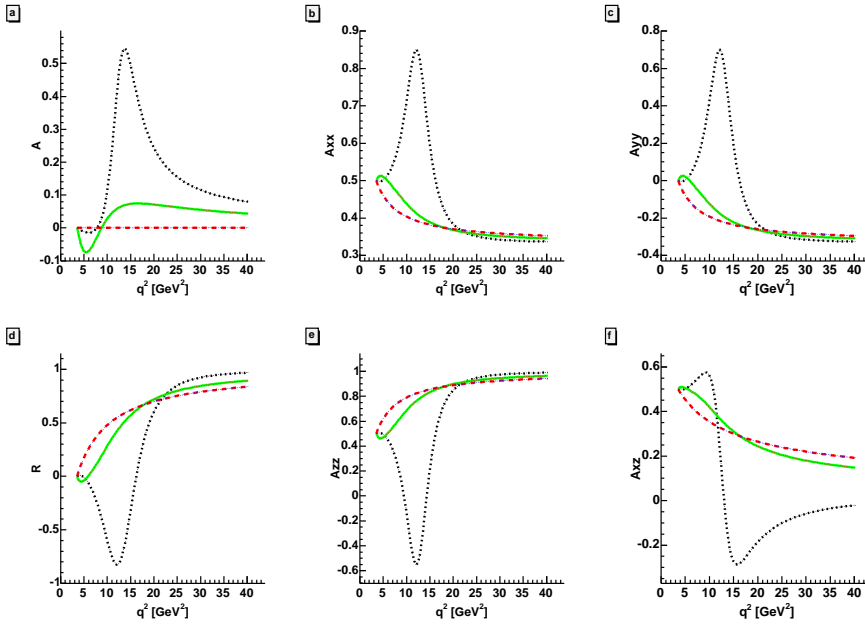


Figure 3. Angular asymmetry and polarization observables, according to Eqs. (8) and (9), for a fixed value of $\theta = 45^\circ$. Notations as in Fig. 2 .

Another problem concerning FFs of pions and nucleons is the large difference in the absolute values in SL and TL regions. For example, at $Q^2=18 \text{ GeV}^2$, the largest value at which proton TL FFs have been measured [7], FFs in TL region differ by a factor of two from the dipole value. The analyticity of FFs allows to apply the Phragmén-Lindelöf theorem [27] which gives a rigorous prescription for the asymptotic behavior of analytical functions:

$$\lim_{t \rightarrow -\infty} F^{(SL)}(t) = \lim_{t \rightarrow \infty} F^{(TL)}(t). \quad (12)$$

This means that, asymptotically, FFs have the following constraints:

1. The time-like phase vanishes: $ImF_i(t) \rightarrow 0$, as $t \rightarrow \infty$;
2. The real part of FFs, in TL region, coincides with the corresponding value in SL region: $ReF^{(TL)}(t)[t \rightarrow \infty] = F^{(SL)}(t)[t \rightarrow -\infty]$, because SL FFs are real functions, due to the hermiticity of the corresponding electromagnetic Hamiltonian.

In order to test the two requirements stated above, the knowledge of the differential cross section for $e^+ + e^- \leftrightarrow p + \bar{p}$ is not sufficient, and polarization phenomena have to be studied also. In this respect, T-odd polarization observables, such as the P_y component of the proton polarization in $e^+ + e^- \rightarrow p + \bar{p}$, are very interesting, although they may be difficult to measure [22].

4 The neutron electric form factor

Let us give a closer look to the neutron electric FF in SL region. The recent measurements are based on the polarization method, and they seem to exceed the Galster parametrization at large Q^2 .

Neutron FFs can also be deduced from the deuteron structure, in the framework of non relativistic IA [28]. The deuteron structure functions can be factorized in a term containing the isoscalar electromagnetic nucleon FFs, G_{ES} , and a term which contains the S- and D-components of the deuteron wave function. The electromagnetic FFs of the nucleons are considered as free ones, without off-shell mass effects.

In Fig. 4 we report the isoscalar nucleon FF, calculated from the experimental data on the structure function $A(Q^2)$ and using the Paris wave function. We illustrate the behavior of the different nucleon electric FFs: G_{ES} , G_{Ep} and G_{En} . G_{ES} , derived from different sets of deuteron data, decreases when Q^2 increases. The solid line represents the Gari-Krümpelmann parametrization [29] for G_{ES} . The dipole behavior, which is generally assumed for the proton electric FF, is shown as a dotted line. The new G_{Ep} data, which decrease faster than the dipole function, are also well reproduced by the Gari-Krümpelmann parametrization (thick dashed line).

The electric neutron FF can be calculated from G_{ES} , assuming for G_{Ep} a dipole behavior (solid stars) or Eq. (1) (open stars). The last option leads to

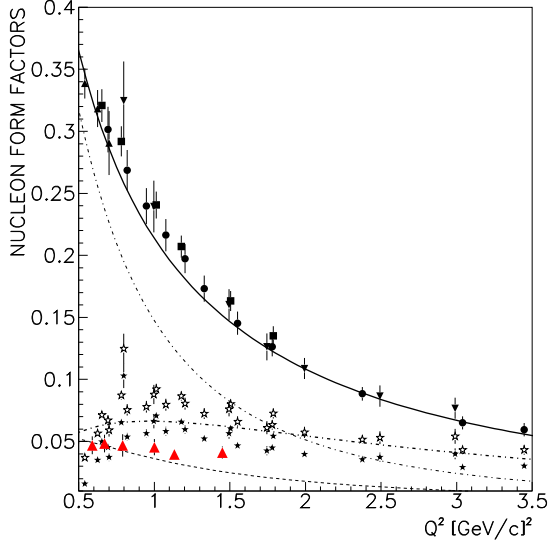


Figure 4. Nucleon electric form factors as functions of the momentum transfer Q^2 in the framework of IA with Paris potential. Isoscalar electric form factors are derived from the deuteron elastic scattering data: Ref. [31] (solid triangles), Ref. [32] (solid circles), Ref. [33] (solid squares), and Ref. [4] (solid reversed triangles). The electric neutron form factors are shown as solid stars when calculated from the dipole representation of G_{Ep} (dotted line) and open stars when G_{Ep} is derived from Eq. (1) (thin dashed-dotted line). The parametrization from Ref. [29] is shown for G_{ES} (solid line) and for G_{En} (thick dashed-dotted line). The thin dashed line is the parametrization from Ref. [30] for G_{En} .

values for G_{En} which are in very good agreement with the parametrization [29]. These results show that G_{En} is not going to vanish at large momentum transfer, but becomes more sizeable than predicted by other parametrizations, often used in the calculations [30] (thin dashed line). Starting from $Q^2 \simeq 2 \text{ GeV}^2$ the form factor G_{En} may become even larger than G_{Ep} .

Recent measurements are reported as solid triangles (for an exhaustive compilation see [34]) and seem to exceed the Galster parametrization at large Q^2 showing a tendency to join the present predictions. Evidently this procedure gives an upper limit for the neutron electric FF, as all other ingredients of the deuteron structure (relativistic corrections, meson exchange currents..) are neglected. So this result suggests that either such corrections are not very large or that they largely cancel. Such description reproduces not only $A(Q^2)$ by construction, but also all other known data on the deuteron, the structure function $B(Q^2)$ and the tensor polarization t_{20} of deuterons scattered by unpolarized

electrons on an unpolarized deuteron target [28].

5 Two-photon exchange

It has been suggested that the discrepancy of the electric form factor data could be at least partly solved by taking into account the two-photon exchange (TPE), in ep elastic scattering (see the talk of L. Pentchev, this conference).

For ep elastic scattering, the one-photon exchange is considered to be the main mechanism. In the standard calculations of radiative corrections [35], the two-photon exchange mechanism is only partially taken into account considering the special part of the integral (the 'box diagrams'), where one photon carries all the momentum transfer and the second photon is almost real. It has been pointed out long ago [36] that, at large momentum transfer, the role of another mechanism, where the momentum transfer is shared between the two photons, can be relatively increased, due to the steep decreasing of the electromagnetic form factors with Q^2 . This effect can eventually become so large that the traditional description of the electron-hadron interaction in terms of electromagnetic currents (and electromagnetic form factors) can become incorrect.

Note that the two-photon exchange should appear at smaller Q^2 for heavier targets: d , ${}^3\text{He}$, ${}^4\text{He}$, because the corresponding form factors decrease faster with Q^2 in comparison with the proton ones. In Ref. [37] the possible effects of 2γ -exchange have been estimated from the precise data on the structure function $A(Q^2)$, obtained at JLab in electron deuteron elastic scattering, up to $Q^2 = 6 \text{ GeV}^2$ [32, 33]. The possibility of 2γ -corrections has not been excluded by this analysis, starting from $Q^2 = 1 \text{ GeV}^2$, and the necessity of dedicated experiments was pointed out. From this kind of considerations, one would expect to observe the two-photon contribution in eN -scattering at larger momentum transfer, for $Q^2 \simeq 10 \text{ GeV}^2$.

The TPE contribution results, first of all, in a nonlocal spin structure of the matrix element. Instead of two real amplitudes, functions of Q^2 , in case of TPE, the matrix element contains three amplitudes $\mathcal{A}_i(s, Q^2)$, $i = 1 - 3$, which are complex functions of two independent variables, s and Q^2 . This makes the analysis of polarization effects quite complicated. The exact calculation of the 2γ -contribution to the amplitude of the $e^\pm p \rightarrow e^\pm p$ -process requires the knowledge of the matrix element for the double virtual Compton scattering, $\gamma^* + p \rightarrow \gamma^* + p$, in a large kinematical region of colliding energy and virtuality of both photons, and can not be done in a model independent form. However, the general symmetry properties of electromagnetic interaction, such as the C-invariance and the crossing symmetry, allow to obtain rigorous results concerning the properties of TPE for elastic eN -scattering and to analyze the effects of this mechanism in eN -phenomenology [38].

The simplest way to measure the TPE contribution needs the parallel study of positron and electron scattering, in the same kinematical conditions. The two-photon contribution cancels (in the first order of the coupling constant α)

in the sum of the differential cross sections, $d\sigma^{(-)}/d\Omega_e + d\sigma^{(+)}/d\Omega_e$. A linear ϵ -fit of this quantity allows to extract $G_E(Q^2)$ and $G_M(Q^2)$, through a generalized Rosenbluth separation. At higher Q^2 , due to the small contribution of $G_E(Q^2)$, the polarization transfer method should be used, which requires the measurement of the P_x and P_z -components of the final nucleon polarization -with longitudinally polarized electron and positron beams. This can be in principle realized at the HERA e^\pm ring, with a polarized jet proton target, and at VEPP3 (Novosibirsk) where experiments are planned.

In absence of positron beam two other possibilities to measure $G_{E,M}(Q^2)$ can be suggested, using only an electron beam [39, 40]. One possibility is the measurement of three T-odd polarization observables, or five T-even polarization observables. All these observables, which vanish in the Born approximation for eN -scattering, must be of the order of α and they should be measured with corresponding accuracy. The extraction of the nucleon electromagnetic FFs is still possible, but requires more complicated experiments, with a very high level of precision. Only in this way it will be possible to investigate the nucleon structure, at large momentum transfer, keeping the elegant formalism of QED, traditionally used for this aim. Therefore, one needs unambiguous experimental evidence of TPE, before advocating the presence of this mechanism, in specific kinematics conditions.

From an analysis of the experimental data, it appears that the available ep elastic scattering cross sections do not show any evidence of deviation from the linearity in the Rosenbluth fit, and hence of the presence of the two-photon contribution, when parametrized following symmetry properties [41].

The new generation of experiments performed at large Q^2 makes use of large acceptance detectors and requires important corrections of the raw data for acceptance, efficiency, energy and angle calibrations [42]. Limits of the procedure and the approximations used for calculating radiative corrections were widely discussed in the literature.

Radiative corrections to the unpolarized cross section may reach 30-40%, whereas they are considered to be negligible in polarization experiments (although one should stress that, in this case, no complete calculation is available). In particular they contain an important ϵ dependence which has a large influence on the slope of the reduced cross section, changing even its sign, as shown in Ref. [41]. It is this slope which is directly related to G_{Ep}^2 . A careful study of the effect of radiative corrections to the experimental data seems necessary, due to their large size and large ϵ dependence, in particular for the large values of ϵ , where the recent experiments have been performed.

Recent measurements of the asymmetry in the scattering of transversely polarized electrons on unpolarized protons give values different from zero, contrary to what is expected in the Born approximation [43, 44]. This observable is related to the imaginary part of the interference between one- and two-photon exchange and can be related only indirectly to the real part of the interference, which plays a role in the elastic ep cross section.

From the theoretical point of view, it seems unavoidable to consider the problem of the TPE contribution in the $\bar{p} + p \rightarrow e^+ + e^-$ reaction (for a complete analysis see Ref. [45]). The process $\bar{p} + p \rightarrow e^+ + e^-$ and its crossing channel, $e + p \rightarrow e + p$, must have common mechanisms.

Particularly interesting is the single-spin asymmetry accessible with a polarized antiproton beam on an unpolarized target, or with an unpolarized antiproton beam on a polarized proton target $A_y(\theta)$, where θ is the angle between the electron and the antiproton momenta in the $\bar{p} + p \rightarrow e^+ + e^-$ reaction CMS.

$A_y(\theta)$ is determined by the spin vector component which is perpendicular to the reaction plane. Being a T-odd quantity, $A_y(\theta)$ does not vanish even in the one-photon-exchange approximation due to the complex nature of the nucleon FFs in the time-like region, in contrast with elastic electron-nucleon scattering.

When the electron is scattered at $\theta = 90^\circ$ in the Born approximation $A_y(\theta)$ vanishes, but the presence of the TPE contributions leads to a non-zero value. This quantity is expected to be small but increasing with q^2 .

6 Conclusions

We have given an overview of the present status of nucleon form factors and presented future developments. Recent data have brought surprises, opened new questions and suggested a different understanding of the nucleon structure. From a theoretical point of view few models give a good description of all four FFs in all kinematical region.

We have shown that in framework of VMD models it is possible to find a general description in all the kinematical domain. Measurements of single spin asymmetry and angular asymmetry in TL region will be very selective on models, as well as double spin observables, which are necessary to fully measure FFs, as they are complex in TL region.

Many questions are still open. Recent data in the SL region show that the ratio G_{Ep}/G_{Mp} deviates from the expected dipole behavior. Experiments will be soon extended until $Q^2=9 \text{ GeV}^2$. The TPE contribution has been suggested to explain this discrepancy, and more experiments are planned in order to sign this mechanism, if present. In the TL region, the values of $|G_M|$ are larger than the corresponding SL values. This has been considered as a proof of the non applicability of the Phr agmen-Lindel of theorem, (up to $s=18 \text{ GeV}^2$, at least) or as an evidence that the asymptotic regime is not reached. The neutron FFs in SL region are far from being negligible even at large Q^2 . In TL region neutron FFs are larger than proton FFs and more experiments are planned at Frascati.

Large progress in view of a global interpretation of the nucleon FFs is expected from future experiments with antiproton beams: it will be possible, at the future FAIR facility at GSI, to separate the electric and magnetic FFs in a wide region of s and to extend the measurement of FFs up to the largest available energy, corresponding to $s \simeq 30 \text{ GeV}^2$. The presence of a large relative phase of magnetic and electric proton FFs in the TL region, if experimentally

proved at relatively large momentum transfer, can be considered a strong indication that these FFs have a different behavior. In particular, it will allow a test of the Phragmen-Lindelöf theorem.

The study of the processes $p + \bar{p} \rightarrow \pi^0 + \ell^+ + \ell^-$ and $p + \bar{p} \rightarrow \pi^+ + \pi^- + \ell^+ + \ell^-$ [46, 47] will allow to measure proton FFs in the unphysical region (for $s \leq 4m^2$, where the vector meson contribution plays an important role) and to determine the relative phase of pion and nucleon FFs.

Acknowledgments

We acknowledge Prof. M. P. Rekaló for fundamental contributions to this subject, for interesting ideas and enthusiastic discussions. We thank C. Duterte et F. Lacroix for their contribution to part of the results presented here.

References

- [1] A. Akhiezer and M. P. Rekaló (1968) *Dokl. Akad. Nauk USSR* **180** 1081; (1974) *Sov. J. Part. Nucl.* **4** 277 ; revised in M. P. Rekaló and E. Tomasi-Gustafsson, Lecture Notes, arXiv:nucl-th/0202025.
- [2] M. K. Jones *et al.* [Jefferson Lab Hall A Collaboration] (2000) *Phys. Rev. Lett.* **84** 1398; O. Gayou *et al.* (2002) *Phys. Rev. Lett.* **88** 092301; V. Punjabi *et al.* (2005) *Phys. Rev. C* **71** 055202.
- [3] M. N. Rosenbluth (1950) *Phys. Rev.* **79** 615.
- [4] R. G. Arnold *et al.* (1986) *Phys. Rev. Lett.* **57** 174;
- [5] R. Madey *et al.* [E93-038 Collaboration] (2003) *Phys. Rev. Lett.* **91** 122002 and refs herein.
- [6] A. Zichichi, S.M. Berman, N. Cabibbo and R. Gatto (1962) *Nuovo Cimento* **XXIV** 170.
- [7] M. Andreotti *et al.* (2003) *Phys. Lett. B* **559** 20 and refs herein.
- [8] A. Antonelli *et al.* (1998) *Nucl. Phys. B* **517** 3.
- [9] F. Iachello, A. D. Jackson and A. Lande (1973) *Phys. Lett. B* **43** 191.
- [10] G. Holzwarth (1996) *Z. Phys. A* **356** 339.
- [11] P. Kroll, M. Schurmann and W. Schweiger (1991) *Z. Phys. A* **338** 339.
- [12] S. Dubnicka, A. Z. Dubnickova, and P. Weisenpacher (2003) *J. Phys. G.* **29** 405; S. Dubnicka, A. Z. Dubnickova arXiv:hep-ph/0401081.
- [13] H.W. Hammer and Ulf-G. Meissner (2004) *Eur. Phys. J. A* **20** 469.
- [14] R. Bijker and F. Iachello (2004) *Phys. Rev. C* **69** 068201.
- [15] E. L. Lomon (2002) *Phys. Rev. C* **66**, 045501.
- [16] G. Hohler, E. Pietarinen, I. Sabba Stefanescu, F. Borkowski, G. G. Simon, V. H. Walther and R. D. Wendling (1976) *Nucl. Phys. B* **114** 505.
- [17] P. E. Bosted (1995) *Phys. Rev. C* **51** 409.
- [18] R. Baldini, C. Bini, P. Gauzzi, M. Mirazita, M. Negrini and S. Pacetti, arXiv:hep-ph/0507085.

- [19] V.A. Matveev, R. M. Muradyan, and A. V. Tavkhelidze (1973) *Lett. Nuovo Cimento* **7** 719; V.L. Chernyak, A. R. Zhitnisky, JETP Lett. 25, 510 (1077); G. P. Lepage and S. J. Brodsky (1980) *Phys. Rev. D* **22** 2157; (1979) *Phys. Rev. Lett.* **43** 545 [Erratum-ibid. (1979) **43** 1625]; A. V. Efremov and A. V. Radyushkin (1980) *Phys. Lett. B* **94** 245.
- [20] M. P. Rekaló and E. Tomasi-Gustafsson (2004) *Eur. Phys. J. A* **22**, 331 and refs herein.
- [21] E. Tomasi-Gustafsson and M. P. Rekaló (2001) *Phys. Lett. B* **504**, 291 and refs herein.
- [22] A. Z. Dubnickova, S. Dubnicka and M. P. Rekaló (1996) *Nuovo Cim. A* **109** 241.
- [23] S. M. Bilenkii, C. Giunti and V. Wataghin *Z. Phys.* **C59**, 475 (1993).
- [24] S. J. Brodsky, C. E. Carlson, J. R. Hiller and D. S. Hwang (2004) *Phys. Rev. D* **69** 054022.
- [25] E. Tomasi-Gustafsson, F. Lacroix, C. Duterte and G. I. Gakh (2005) *Eur. Phys. J. A* **24** 419
- [26] A. V. Belitsky, X. d. Ji and F. Yuan (2003) *Phys. Rev. Lett.* **91**, 092003.
- [27] E. C. Titchmarsh (1939) *Theory of functions* (Oxford University Press, London).
- [28] E. Tomasi-Gustafsson and M. P. Rekaló (2001) *Europhys. Lett.* **55** 188.
- [29] M. Gari and W. Krümpelmann (1992) *Phys. Lett. B* **274** 159.
- [30] S. Galster, H. Klein, J. Moritz, K. H. Schmidt, D. Wegener and J. Bleckwenn (1971) *Nucl. Phys. B* **32** 221.
- [31] S. Platchkov *et al.* (1990) *Nucl. Phys A* **510** 740 .
- [32] L. C. Alexa *et al.* (1999) *Phys. Rev. Lett.* **82** 1374.
- [33] D. Abbott *et al.* [The t_{20} collaboration] (1999) *Phys. Rev. Lett.* **82** 1379.
- [34] M. Seimetz [for the A1 collaboration] (2005) *Nucl. Phys. A* **755** 231c.
- [35] L. W. Mo and Y. S. Tsai (1969) *Rev. Mod. Phys.* **41** 205.
- [36] J. Gunion and L. Stodolsky (1973) *Phys. Rev. Lett.* **30** 345; (1973) V. Franco *Phys. Rev. D* **8** 826; (1973) V. N. Boitsov, L.A. Kondratyuk and V.B. Kopeliovich *Sov. J. Nucl. Phys.* **16** 237; (1973) F. M. Lev *Sov. J. Nucl. Phys.* **21** 45.
- [37] M. P. Rekaló, E. Tomasi-Gustafsson and D. Prout (1999) *Phys. Rev.* **C60** 042202.
- [38] M. P. Rekaló and E. Tomasi-Gustafsson (2004) *Eur. Phys. J. A.* **22** 331.
- [39] M. P. Rekaló, E. Tomasi-Gustafsson (2004) *Nucl. Phys. A* 740 271.
- [40] M. P. Rekaló, E. Tomasi-Gustafsson (2004) *Nucl. Phys. A* 742 322.
- [41] E. Tomasi-Gustafsson and G. I. Gakh, (2004) arXiv:hep-ph/0412137, to appear in *Phys. Rev. C*.
- [42] M. E. Christy *et al.* [E94110 Collaboration], (2004) *Phys. Rev. C* **70** 015206.
- [43] S. P. Wells *et al.* [SAMPLE collaboration], (2001) *Phys. Rev. C* **63** 064001.
- [44] F. E. Maas *et al.* (2005) *Phys. Rev. Lett.* **94** 082001.
- [45] G. I. Gakh and E. Tomasi-Gustafsson (2005) arXiv:nucl-th/0504021 to appear in *Nucl. Phys. A*.
- [46] M. P. Rekaló, *Sov. J. Nucl. Phys.* **1**, 760 (1965) [*J. Nucl. Phys. (USSR)* **1**, 1066 (1965)].
- [47] A. Z. Dubnickova, S. Dubnicka and M. P. Rekaló, *Z. Phys. C* **70**, 473 (1996).